Calculations of thermophysical properties of cubic carbides and nitrides using the Debye–Grüneisen model

Xiao-Gang Lu *, Malin Selleby, Bo Sundman

Department of Materials Science and Engineering, Royal Institute of Technology, SE-100 44 Stockholm, Sweden

Abstract

The thermal expansivities and heat capacities of MX (M = Ti, Zr, Hf, V, Nb, Ta; X = C, N) carbides and nitrides with NaCl structure were calculated using the Debye–Grüneisen model combined with ab initio calculations. Two different approximations for the Grüneisen parameter γ were used in the Debye–Grüneisen model, i.e. the expressions proposed by Slater and by Dugdale and MacDonald. The thermal electronic contribution was evaluated from ab initio calculations of the electronic density of states. The calculated results were compared with CALPHAD assessments and experimental data. It was found that the calculations using the Dugdale–MacDonald γ can account for most of the experimental data. By fitting experimental heat capacity and thermal expansivity data below the Debye temperatures, an estimation of Poisson's ratio was obtained and Young's and shear moduli were evaluated. In order to reach a reasonable agreement with experimental data, it was necessary to use the logarithmic averaged mass of the constituent atoms. The agreements between the calculated and the experimental values for the bulk and Young's moduli are generally better than the agreement for shear modulus.

Keywords: Heat capacity; Thermal expansivity; Ab initio calculations; Debye–Grüneisen model; Elastic modulus

1. Introduction

Transition metal carbides and nitrides are extensively studied experimentally and theoretically [1–7] due to their excellent thermophysical properties [1,2], such as hardness, high melting temperature, good chemical and mechanical stability, and high thermal conductivity. Numerous experimental investigations have been published, and hence a fundamental physical picture has been established. However, due to the experimental difficulties arising from various factors, such as composition control, porosity, impurities, etc., the experimental data are largely scattered. On the other hand, ab initio calculations of the thermophysical properties are very time-consuming.

In a previous article [8], following the work by Wang et al. [9], we derived a general relation between the Debye temperature and the volume. This relation, equivalent to the expression proposed by Wang et al. [9], was then used in the Debye–Grüneisen model to calculate the coefficient of thermal linear expansion (CLE) of metallic elements with cubic structures. Comparison with experimental data shows that this general relation, when incorporated in the Debye–Grüneisen model, accounts well for the experimental data.

In the present work, we extend the same method to calculate CLE and heat capacity of group IV and V transition metal carbides and nitrides with NaCl structure at the stoichiometric composition. Comparing the calculated results with experimental data, it was found to be possible to estimate a value for Poisson's ratio which can be used to estimate Young's and shear moduli.

* Corresponding author. Tel.: +46 8 54595937.
E-mail address: xiaogang@thermocalc.se (X.-G. Lu).

doi:10.1016/j.actamat.2006.05.054

2. Methodology

2.1. Assessment of experimental data

As mentioned above, experimental measurements on carbides and nitrides are difficult, and the measured data are not always consistent. In order to make a valid comparison between the Debye–Grüneisen calculations and experimental data, it is necessary to assess critically the experimental results.

2.1.1. Heat capacity

Storms [1] presented in 1967 an early study of various carbides and listed the heat capacity data. Later compilations of thermodynamic properties, known as JANAF data [10], were based on critical reviews of experimental measurements covering publications until 1985.

CALPHAD modeling [11,12] has nowadays become a mature and powerful method for the study of thermodynamic properties of complex systems. Thermodynamic models are assigned to all phases and model parameters are assessed using all kinds of experimental data simultaneously yielding a consistent thermodynamic description of the system. Inconsistent experimental data are easily detected in such an assessment procedure. At present, most of the carbon- and nitrogen-containing systems covered in this work have been assessed using the CALPHAD method. The most recent descriptions were used to calculate heat capacity to be compared with the Debye–Grüneisen calculations. No thermodynamic reassessment was performed in the present work.

2.1.2. CLE

Touloukian et al. [13] compiled the results from the major experimental investigations published before 1973 and listed recommended values for the macroscopic linear expansion ($\Delta L/L_0$) and CLE up to the melting points of the materials concerned. This information is referred to as TPRC data in the following discussion.

In the literature, there are large amounts of X-ray or neutron diffraction measurements of lattice parameters, and they are usually of high precision. One of the early collections was edited by Pearson [14]. In the present work, new published data were collected and critically reviewed. The lattice parameter data were converted to volume data and then adopted in the CALPHAD assessments using the PARROT module [15] in the Thermo-Calc software package [16,17]. In general, the assessed CLEs in the present work are in good agreements with the TPRC data.

2.2. Ab initio calculations

In this work, ab initio electronic total energy calculations were performed within the framework of the density functional theory (DFT) using the Vienna Ab initio Simulation Package (VASP) [18,19]. The carbides and nitrides with NaCl structure at their stoichiometric compositions were considered. The total energy and volume relation (i.e. equation of state, EOS) at 0 K can be obtained by performing a series of calculations at different volumes, followed by fitting to a Morse function. From the fitting, the equilibrium volume, bulk modulus and other necessary values needed in the Debye–Grüneisen model can be easily obtained. The electronic density of states (DOS), which must be known when evaluating electronic contributions at finite temperatures, can also be obtained from the VASP calculations.

The standard projected augmented wave (PAW) potentials [20] provided with VASP were used, and the Perdew–Wang version of the generalized gradient approximation (GGA-PW91) [21,22] was adopted. A $16\times\ 16\times 16k$-point mesh was chosen. A cutoff energy of 520 eV was used for all the calculations for carbides and nitrides. The smearing method is the tetrahedron method with Blöchl corrections.

2.3. Debye–Grüneisen model

When the Helmholtz energy, F, is expressed as function of T and V, the equilibrium $V(T)$ and thus CLE can be calculated by finding the minimum of $F(T,V)$ at each temperature. In addition, heat capacity and entropy, as well as other thermodynamic properties can be calculated once the equilibrium volume is determined. In calculating the total Helmholtz energy, the vibrational contribution is a major issue. The Debye–Grüneisen model has long been used to describe the behavior of vibrating lattices, and is capable of accounting for anharmonic effects. The details of the method were discussed in a previous paper [8] and the following is only a brief summary.

2.3.1. Total Helmholtz energy

We consider a system of 1 mol of formula units of the compound A_1B_1 which contains $N=2N_A$ atoms (N_A is Avogadro's number). The total Helmholtz energy of the system comprises the total energy from ab initio electronic total energy calculations at $T=0$ K, E_{tot}, the free energy of the vibrating lattice, F_D, and the contribution due to the thermal excitations of electrons, F_{el}:

$$F(T,V)=E_{tot}(V)+F_D(T,V)+F_{el}(T,V)=E_{tot}(V)+E_D(T,V)-TS_D(T,V)+E_{el}(T,V)-TS_{el}(T,V) \quad (1)$$

The electronic energy due to thermal electronic excitations, i.e. the energy increase of the electrons when heated from 0 to T, can be expressed as [23]:

$$E_{el}(T,V)=N_A\int_{-\infty}^{\infty} n(\varepsilon,V)f(\varepsilon,T)\varepsilon\,d\varepsilon-N_A\int_{-\infty}^{\varepsilon_F} n(\varepsilon,V)\varepsilon\,d\varepsilon \quad (2)$$

where $n(\varepsilon,V)$ is the electronic DOS, and $f(\varepsilon,T)$ represents the Fermi–Dirac distribution. The electronic entropy is formulated as [24]:

$$S_{el}(T,V) = -N_A k_B \int_{-\infty}^{\infty} n(\varepsilon,V)[f(\varepsilon,T)\ln f(\varepsilon,T) + (1-f(\varepsilon,T))\ln(1-f(\varepsilon,T))]d\varepsilon \quad (3)$$

The DOS is calculated at 0 K for each volume, and numerically integrated with respect to energy, ε, according to Eqs. (2) and (3). In practice, the integration is performed adequately in the vicinity of the Fermi energy since the temperatures studied are far below ε_F/k_B. Then the electronic energy and entropy obtained are used in Eq. (1). The electronic excitations are not negligible for many materials, especially at high temperatures near the melting point.

2.3.2. Calculation of the free energy of a vibrating lattice, $F_D(T,V)$

Three well-known approximations to account for the Grüneisen parameter γ can be combined into the following expression [25,26]:

$$\gamma(V) = \frac{1}{3}(\lambda-1) - \frac{V}{2}\frac{\partial^2\left[PV^{(2/3)(\lambda+1)}\right]/\partial V^2}{\partial\left[PV^{(2/3)(\lambda+1)}\right]/\partial V} \quad (4)$$

where

$$P(V) = -\frac{\partial E(V)}{\partial V}$$

When $\lambda = -1$, 0 and +1, one obtains the Slater approximation [27], Dugdale–MacDonald (DM) approximation [28] and the expression resulting from the free volume theory [29], respectively. When integrating

$$\gamma(V) = -\frac{\partial \ln \theta_D}{\partial \ln V}$$

from both sides and using Eq. (4), one obtains

$$\theta_D(V) = AV^{2/3}\left[-\frac{\partial P(V)}{\partial V} - \frac{2(\lambda+1)}{3}\frac{P(V)}{V}\right]^{1/2} \quad (5)$$

where A is the integral constant that is determined as described below.

The Debye temperature is proportional to the sound velocity, v_D (see, e.g. Ref. [30]):

$$\theta_D(V) = \frac{\hbar}{k_B}\left(\frac{6\pi^2 N}{V}\right)^{1/3} v_D = \frac{\hbar}{k_B}\left(\frac{6\pi^2 r N_A}{V}\right)^{1/3} v_D \quad (6)$$

where

$$v_D = k(v)\sqrt{\frac{B}{\rho}} = k(v)\sqrt{\frac{VB}{rm}} \quad (7)$$

and

$$k(v) = \left\{\frac{2}{3}\left[\frac{2(1+v)}{3(1-2v)}\right]^{3/2} + \frac{1}{3}\left[\frac{1+v}{3(1-v)}\right]^{3/2}\right\}^{-1/3} \quad (8)$$

where v is Poisson's ratio, ρ is the density, r is the number of atoms in the chemical formula of the material ($r = 1$ for an element, 2 for cubic carbides and nitrides) and B is the bulk modulus. The mass, m, is an effective atomic mass defined as the logarithmic average of all masses in the formula [30]. For cubic carbides and nitrides A_1B_1, m is calculated by

$$\ln(m) = \frac{1}{2}\ln(m_A) + \frac{1}{2}\ln(m_B)$$

The choice of the logarithmic average of mass, instead of the arithmetic average, is essential to account for Poisson's ratio for materials with large differences in atomic masses, such as TaC and HfC. Fig. 1 demonstrates the effect of the average mass on the calculated heat capacity of TaC. For CLE, the influence is very similar. Using the definition of B, one can derive

$$\theta_D(V) = k(v)\frac{\hbar}{k_B}\left(\frac{6\pi^2 N}{V}\right)^{1/3}\left[\frac{-V^2\frac{\partial P(V)}{\partial V}}{rm}\right]^{1/2} = k(v)\frac{\hbar}{k_B\sqrt{rm}}\left(6\pi^2 N\right)^{1/3}V^{2/3}\left[-\frac{\partial P(V)}{\partial V}\right]^{1/2} \quad (9)$$

On the other hand, when $\lambda = -1$, i.e. Slater's expression is chosen, Eq. (5) reduces to

$$\theta_D(V) = AV^{2/3}\left[-\frac{\partial P(V)}{\partial V}\right]^{1/2} \quad (10)$$

Comparing Eqs. (9) and (10), the constant A is identified as

$$A = k(v)\frac{\hbar}{k_B\sqrt{rm}}\left(6\pi^2 N\right)^{1/3} \quad (11)$$

Inserting it back into Eq. (5), we obtain

$$\theta_D(V) = k(v)\frac{\hbar}{k_B\sqrt{rm}}\left(6\pi^2 N\right)^{1/3}V^{2/3} \times \left[-\frac{\partial P(V)}{\partial V} - \frac{2(\lambda+1)}{3}\frac{P(V)}{V}\right]^{1/2} \quad (12)$$

This is the general θ_D–V relation. When the approximation for the Grüneisen parameter γ is chosen, the value in the square brackets in Eq. (12) can be evaluated thoroughly

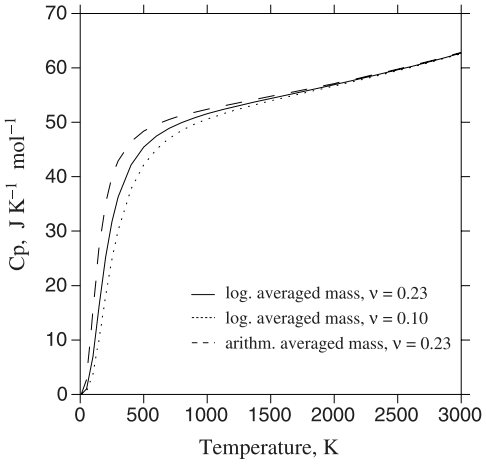

Fig. 1. Influences of mass and Poisson's ratio on the heat capacity of TaC. The influences on CLE are similar.

from ab initio calculations at 0 K. Poisson's ratio, v, and mass are two important properties. Their significance will be discussed in the following sections.

Using Eq. (12) in the Debye formula, the vibrational energy and entropy are expressed as functions of volume and temperature as follows:

$$E_{\mathrm{D}}(T,V) = \frac{9}{8}Nk_{\mathrm{B}}\theta_{\mathrm{D}} + 3Nk_{\mathrm{B}}TD\left(\frac{\theta_{\mathrm{D}}}{T}\right) \tag{13}$$

$$S_{\mathrm{D}}(T,V) = 3Nk_{\mathrm{B}}\left[\frac{4}{3}D\left(\frac{\theta_{\mathrm{D}}}{T}\right) - \ln\left(1-\mathrm{e}^{-\theta_{\mathrm{D}}/T}\right)\right] \tag{14}$$

where $D(\theta_{\mathrm{D}}/T)$ denotes the Debye function.

2.4. Estimation of elastic moduli

As demonstrated in Fig. 1, Poisson's ratio v, and hence $k(v)$, has very little effect on the calculated CLE and heat capacity at high temperatures. However, below the Debye temperature, its effect is apparent and cannot be ignored. It is possible to fit the experimental data for heat capacity and CLE around the Debye temperature by just changing the value of Poisson's ratio. Here the role played by Poisson's ratio is a fitting parameter and the method is therefore semi-empirical. The resulting Poisson's ratio is considered to be an average value for isotropic polycrystalline materials.

The bulk modulus B at 0 K can be calculated directly from the ab initio results. Once the bulk modulus and Poisson's ratio are known, Young's modulus, E, and shear modulus, G, can be evaluated:

$$E = 3B(1-2v) \tag{15}$$

$$G = \frac{3B(1-2v)}{2(1+v)} = \frac{E}{2(1+v)} \tag{16}$$

3. Results and discussion

3.1. CLE and heat capacity

Comparisons between calculations using the Debye–Grüneisen model and CALPHAD assessments as well as experimental data are presented in Figs. 2–12. In this work, both Slater's and the DM expressions for γ are used. As one can see in these plots, the DM approximation usually sets the lower limit for CLE and heat capacity. The calculated properties according to the free volume theory [29], which gives even lower values, are not shown in the figures and are not discussed in this paper.

The calculated CLEs using Slater's and the DM approximations differ largely even below room temperature. On the contrary, the calculated heat capacity does not show a noticeable difference until the temperature is approximately above Debye temperature.

In the following, a detailed discussion for each individual carbide and nitride is presented.

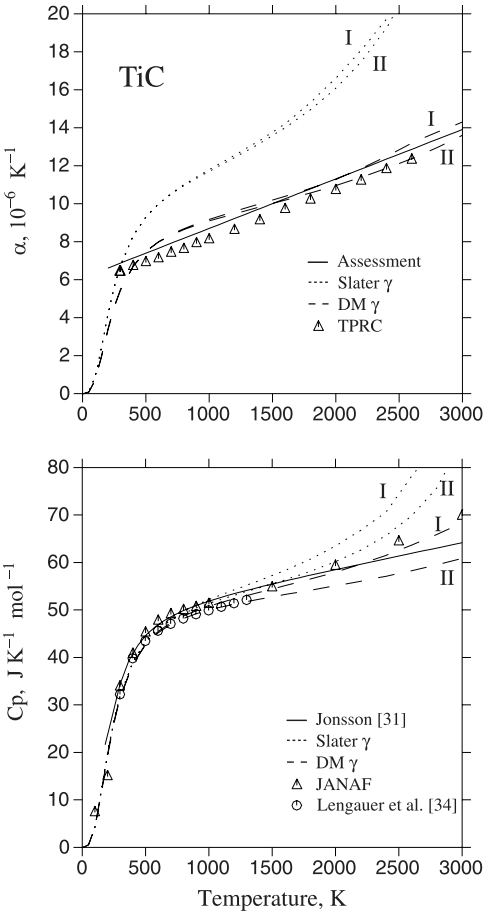

Fig. 2. Calculated CLE and C_p compared with the experimental data for cubic TiC. Curve I: with electronic contributions; curve II: without electronic contributions.

3.1.1. TiC and TiN

Jonsson performed CALPHAD assessments of the heat capacities of stoichiometric TiC [31] and TiN [32]. His results were reviewed and accepted in a recent reassessment of the Ti–C–N system by Dumitrescu et al. [33]. However, at high temperatures, the assessed data are lower than the JANAF data, especially for TiN (Figs. 2 and 3). More recent measurements of the heat capacity of TiN by Lengauer et al. [34] show a similar trend to the JANAF data at elevated temperatures. The assessed CLE is based on the lattice parameter data reported recently by Aigner et al. [35], Wokulska [36] and Dubrovinskaia et al. [37].

In Fig. 2, the calculated heat capacity and CLE of TiC with both Slater's and the DM values of γ are shown. The electronic contribution to the CLE is quite small, while the electronic heat capacity is not negligible. The calculation with the DM γ agrees well with JANAF data for both TiC and TiN.

3.1.2. ZrC and ZrN

The Zr–C system was assessed by Guillermet [38]. The assessed C_p agrees with the JANAF data at high tempera-

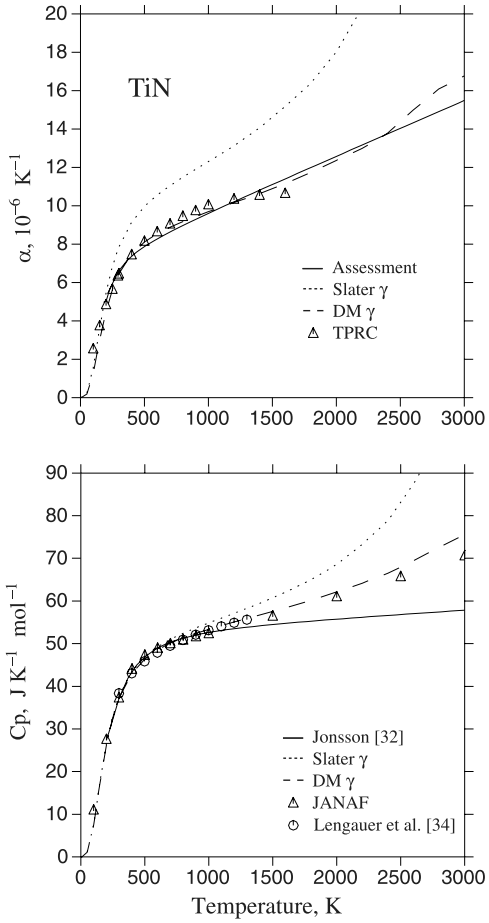

Fig. 3. Calculated CLE and C_p compared with the experimental data for cubic TiN.

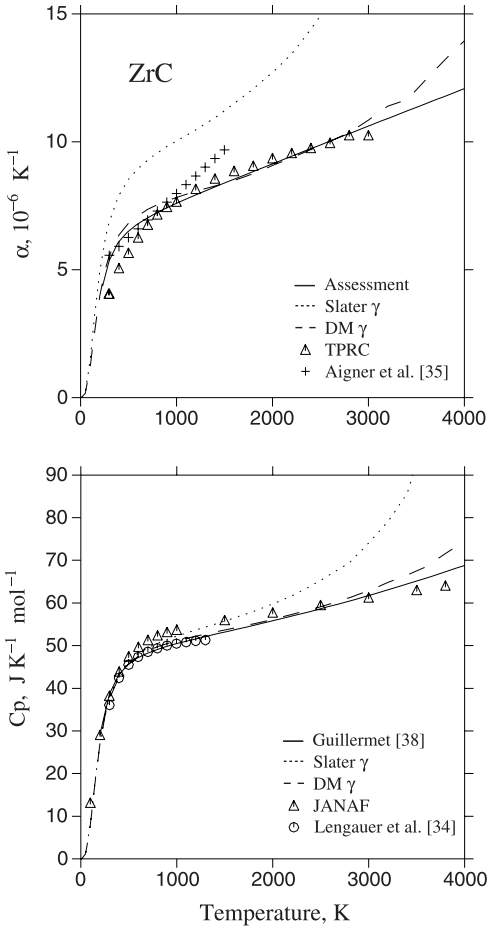

Fig. 4. Calculated CLE and C_p compared with the experimental data for cubic ZrC.

tures above 2000 K, and Storms' tabulated data [1] between 1000 and 2000 K, as well as the measurements of Lengauer et al. [34]. The calculated heat capacity with the DM γ is very close to that of the assessment.

For the CLE of ZrC, our calculation cannot reproduce the TPRC data below 1000 K, whereas it is in good agreement with Aigner et al. [35]. However, for both ZrC and ZrN, the CLE data seem problematic at the highest temperatures reported by Aigner et al. [35].

For ZrN, the calculations with the DM γ are in good agreement with TPRC and JANAF data.

3.1.3. HfC and HfN

The assessments of the CLEs of HfC and HfN are mainly based on the recent measurement by Aigner et al. [35]. However, their measured CLEs contradict earlier measurements. Our calculated CLE using the DM γ, however, agrees well with TPRC data for HfC and with data from Bogdanov et al. [39] for HfN.

3.1.4. VC and VN

The highest carbon content in cubic VC_{1-x} is $x \approx 0.1$. The CLE was assessed using the lattice parameters of $VC_{0.89}$ measured by Storms and Kempter [43], for which the measurement was performed below 900 K. They also observed that the average CLE decreases with increasing carbon content. Hence, the CLE for the metastable stoichiometric VC may be lower than the present assessment. The limited experimental data only allow fitting using a linear function for CLE. The assessed CLE agrees reasonably with the Debye–Grüneisen calculation, while the TPRC data are much lower.

For the heat capacity of VC, Lipatnikov et al. [44] studied the order–disorder phase transformation in non-stoichiometric vanadium carbide, and measured the heat capacities. They observed that the heat capacity increased with increasing carbon content, and decreased due to ordering. In Fig. 8, the experimental data for $VC_{0.87}$ are compared with the calculated and assessed [45] heat capacity. The agreement is good bearing in mind that the present calculation was performed for stoichiometric VC.

Lengauer and Ettmayer [46] measured the lattice parameters of VN_{1-x} between 298 and 1000 K, and concluded that the nitrogen content does not influence the CLE of VN_{1-x}. In this work, the CLE of stoichiometric VN was determined using the lattice parameters of $VN_{0.996}$. The assessment is in accordance with the measurement by Bogdanov et al. [39] for $VN_{0.93}$.

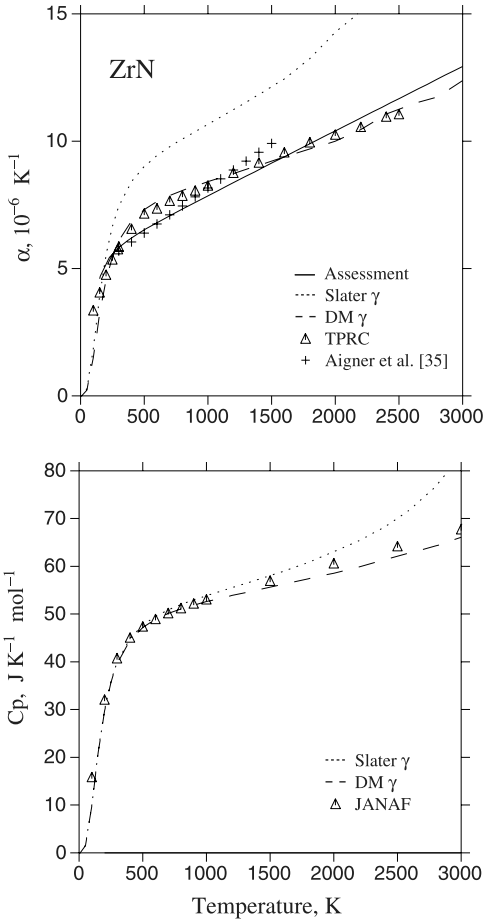

Fig. 5. Calculated CLE and C_p compared with the experimental data for cubic ZrN.

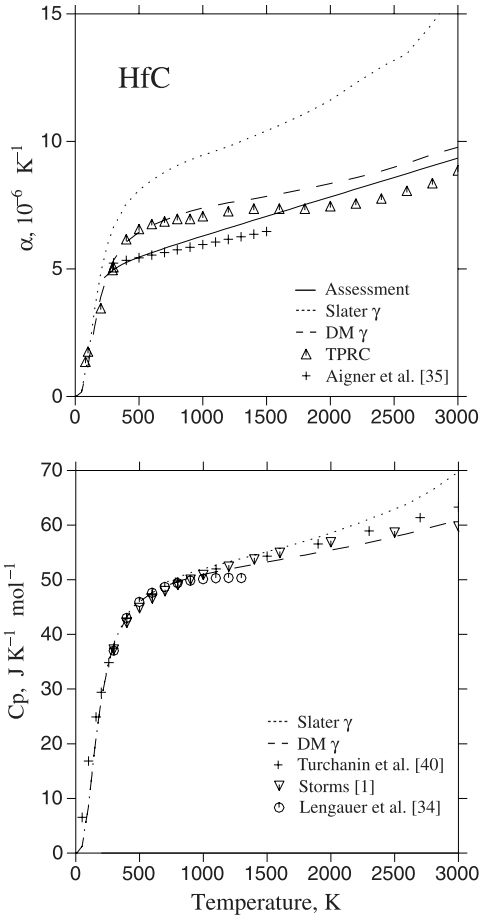

Fig. 6. Calculated CLE and C_p compared with the experimental data for cubic HfC. See above-mentioned references for further information.

Carlson et al. [47] presented a critical review of the thermodynamic data for the *V–N* system prior to 1986. The heat capacity was fitted using the latest experimental data reported by Litvinenko et al. [48], and agrees well with JANAF data. A more recent assessment by Du et al. [49] was based on these data. However, these results for heat capacity are lower than our calculated values. This is rather unusual because as can be seen from Figs. 2–12, the calculation with the DM γ reproduces most of the heat capacity data. The other unusual case is NbN, for which only a few experimental heat capacity measurements are available.

3.1.5. NbC and NbN

The calculations of thermal electronic contributions of NbC and NbN are not as successful as the calculations for most other carbides and nitrides studied in this work. As observed from the calculated results, the DOS of NbC and NbN are unusually high, very close to the Fermi energy. Since the numerical integration is used to calculate the electronic energy and entropy according to Eqs. (2) and (3), an improper integration interval may cause numerical problems near the Fermi energy. A slightly non-smooth CLE curve for ZrC is also observed in Fig. 4. In this work, the problem has not been successfully solved, but it is necessary to carry out further investigations of the DOS calculations for NbC and NbN as well as an improvement of the integration algorithm. As a rough approximation, the DOS of TaC and TaN were used for those of NbC and NbN, respectively. This may not be a bad approximation, as we noticed that the thermal electronic contribution has the same magnitude for most carbides and nitrides studied in this work. This approximation will not affect the results for the elastic properties since the electronic contribution is very small below the Debye temperature (see Fig. 2).

Kempter and Storms [50] reported thermal expansion measurements of $NbC_{0.702}$, $NbC_{0.766}$, $NbC_{0.825}$ and $NbC_{0.924}$. They concluded that the average CLE increases with increasing carbon content, which is not the case for VC. Huang and Selleby [51] assessed the heat capacity of NbC as well as the whole Nb–C system. The present calculation agrees well with their assessment and with low-temperature measurements of heat capacity by Gusev et al. [52].

Lengauer and Ettmayer [53] measured the lattice parameters of three NbN_{1-x} samples from 298 to 1100 K. The assessed CLE was based on their lattice parameters of $NbN_{0.975}$. However, Bogdanov et al. [39] reported a lower

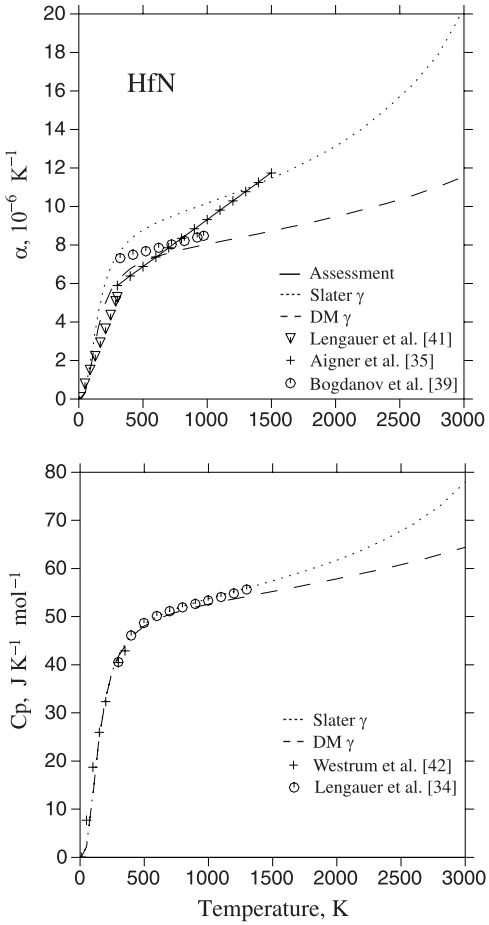

Fig. 7. Calculated CLE and C_p compared with the experimental data for cubic HfN. See above-mentioned references for further information.

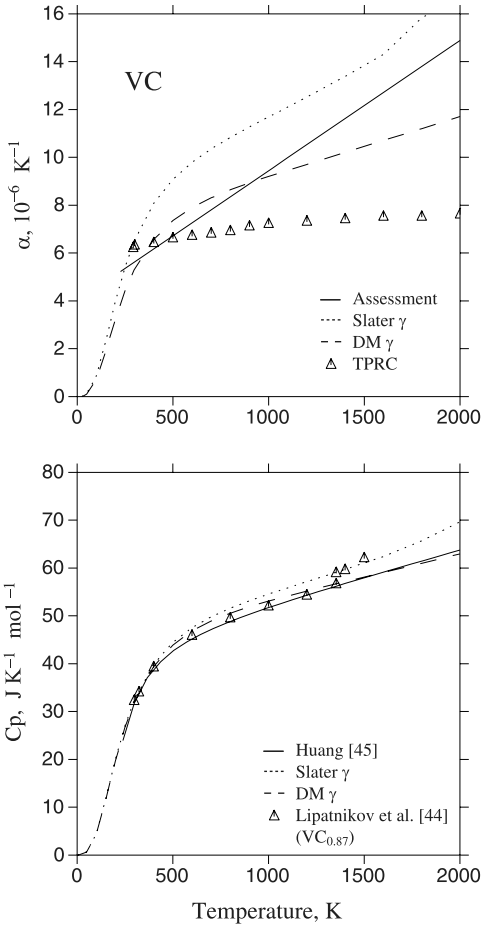

Fig. 8. Calculated CLE and C_p compared with the experimental data for cubic VC.

CLE of $NbN_{0.99}$, and Timofeeva and Shvedova [54] gave a value of $4.3 \times 10^{-6}\,K^{-1}$ for the average CLE of $NbN_{0.95}$ below 300 K. In this work, it is found that most calculations with the DM γ agree better with the experimental data than those using Slater's γ. Lengauer and Ettmayer's experiment for NbN is an exception and further measurements are needed to provide confirmation.

Based on a few rough estimations of heat content and entropy, Huang [55] assessed the heat capacity of NbN. Since no experimental data on the heat capacity were used, the assessed data may not be reliable. By comparing with the calculated heat capacity from optical spectra measurements by Kutolin et al. [56], it is shown in Fig. 11 that the assessed heat capacity at 298 K is higher than this value.

3.1.6. TaC

Frisk and Guillermet [57] assessed the Ta–C system and their assessed heat capacity of TaC agrees well with JANAF data. In this work, TaN is not calculated using the Debye–Grüneisen model since no experimental information can be found to make a comparison. Only the bulk modulus is calculated at 0 K and compared with other ab initio calculations.

3.2. Debye temperature and Poisson's ratio

Although Poisson's ratio seems to have negligible temperature dependence (e.g. for NbC and TaC [58]) and negligible porosity dependence (e.g. for TiC and TaC [59]), experiments are still difficult and measured data largely scattered. This situation motivates numerous theoretical studies as well as the present calculation. The evaluated Poisson's ratio and Debye temperature are listed in Table 1. They are generally larger than the experimental data [56,58–64], but still in reasonable agreement.

The use of logarithmic averaged mass is essential to deal with TaC, HfC and HfN, for which the constituent atoms have very different atomic masses. As shown in Table 1, the fitted Poisson's ratios for HfC and HfN with arithmetic averaged mass are 0.08 and 0.14, respectively, which are much lower than the measurements. Since the logarithmic averaged mass is lower than the corresponding arithmetic averaged mass, the consequence is that the resulting Debye temperature is increased according to Eq. (12). In order to fit the experimental data, higher Poisson's ratio (hence lower $k(v)$) is needed to compensate for the effect of the increased Debye temperature due to the logarithmic averaged mass. For HfC and HfN, the fitted Poisson's ratios

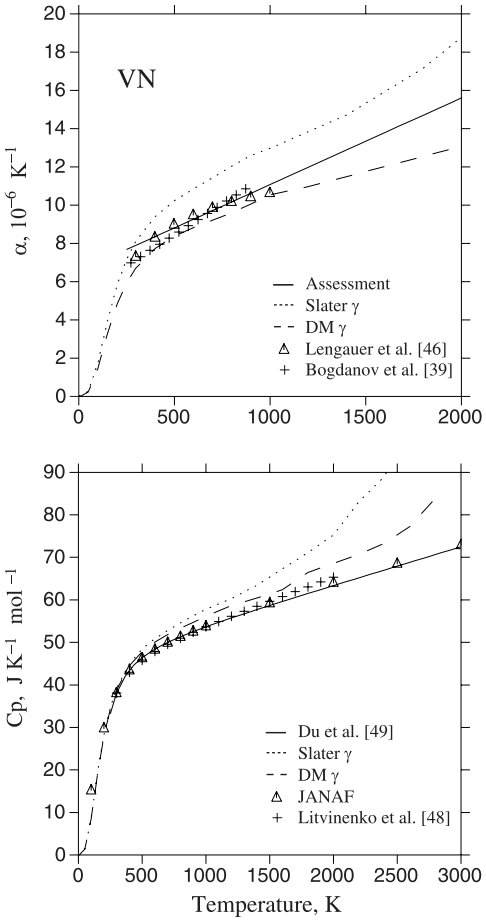

Fig. 9. Calculated CLE and C_p compared with the experimental data for cubic VN.

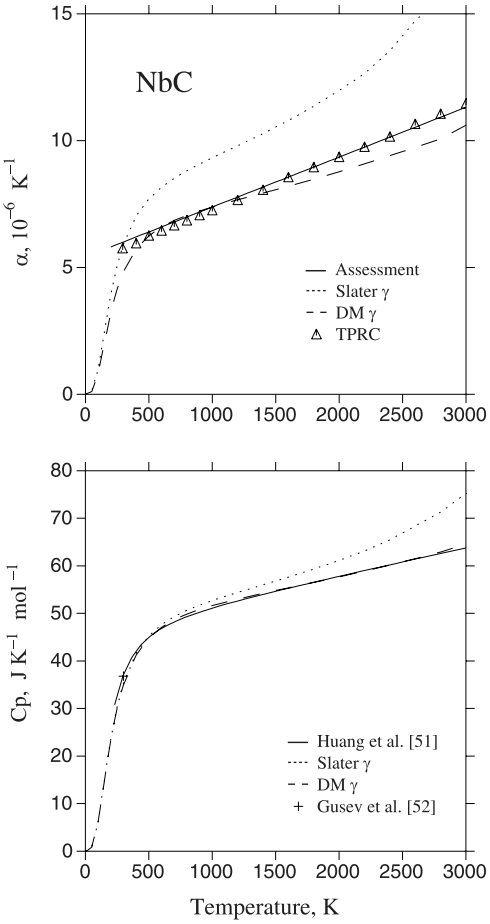

Fig. 10. Calculated CLE and C_p compared with the experimental data for cubic NbC.

for logarithmic averaged mass become 0.215 and 0.30, respectively. In contrast, for the compounds that have similar values for the two averaged masses, such as TiC and TiN, the differences of the results with both averaged masses are less dramatic. In general, using the logarithmic averaged mass produces better results as shown in Table 1. Therefore only calculations using this averaged mass are discussed in the following sections.

Strictly speaking, the Debye–Grüneisen model only accounts reasonably for the low-frequency part of the phonon spectrum, and the calculated thermophysical properties agree with the experiments at very low temperatures. For the complex high-frequency phonon spectrum, the Debye approach is a rough approximation and makes considerable simplifications. However, for certain thermophysical properties, certain averages of the phonon frequencies may be sufficient to capture the essential features of the lattice vibrational contributions [30]. This is demonstrated in the above calculations of heat capacity and CLE. However, the method used in the present work to obtain Poisson's ratio may introduce errors, because the experimental data around the Debye temperature are the primary inputs and at the Debye temperature all phonon modes are excited. This may be one of the reasons that the calculated Poisson's ratios deviate from the experimental data.

3.3. Elastic properties

The calculated elastic moduli using the logarithmic averaged mass are listed in Table 2, as well as the experimental data at room temperature. The calculated bulk moduli agree well with the experimental data, whereas the calculated shear moduli are less satisfactory. The agreement for Young's modulus is between that of the bulk modulus and the shear modulus. This may be explained by the fact that calculations of both E and G involve Poisson's ratio and the calculated Poisson's ratios are generally larger than the experimental data. According to Eq. (15), Young's modulus E is a linear function of Poisson's ratio and is lower than the experimental data due to the higher calculated value of Poisson's ratio. According to Eq. (16), the accumulated error from E and v will result in even lower values of shear modulus G.

In general, the agreements are better for carbides than for nitrides. The worst case is for TiN, for which the calculated Young's modulus is about 60% lower than the most recent measurements by Kim et al. [61] and Yang et al. [66]. However, Poisson's ratio deduced from the measurements of B and G by Yang et al. is 0.22, which is lower than

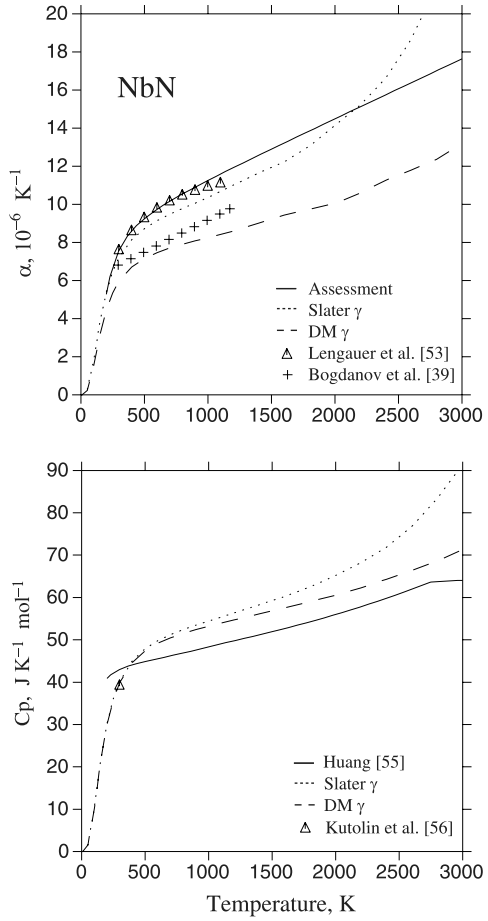

Fig. 11. Calculated CLE and C_p compared with the experimental data for cubic NbN.

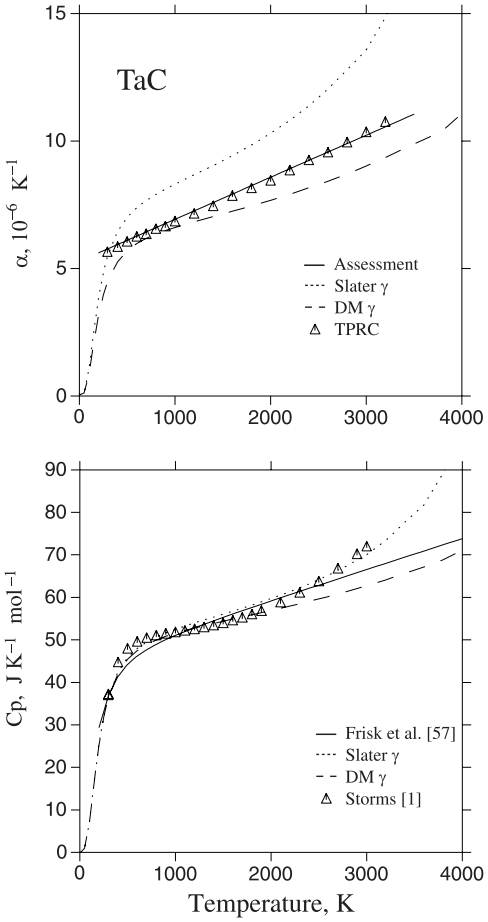

Fig. 12. Calculated CLE and C_p compared with the experimental data for cubic TaC.

those of other experiments (0.254 and 0.295). Similarly, Poisson's ratio for HfN (0.17) is also lower than other measured values (0.259–0.35).

Since the experimental data are largely scattered, it is beneficial to compare the results calculated in this work with the values obtained directly from ab initio

Table 1
The calculated Debye temperature and Poisson's ratio using two different averaged masses, i.e. logarithmic averaged mass and arithmetic averaged mass

	θ (Calculated) (K)		θ (Experiment) (K)	Poisson's ratio (calculated)		Poisson's ratio (experiment)
	Logarithmic mass	Arithmetic mass		Logarithmic mass	Arithmetic mass	
VC	971	913	–	0.265	0.24	0.19–0.32 [60]
VN	755	727	772 [56]	0.346	0.33	0.256 [61][a]
NbC	860	779	742, 761 [62]; 754 [63]	0.255	0.19	0.22 [64]; 0.209–0.23 [60]; 0.21 [58]
NbN	689	721	730 [56]	0.325	0.23	0.275 [61][a]
TaC	808	689	573, 616 [62]; 593 ± 71 [59]	0.23	0.125	0.24 [64]; 0.172–0.24 [60]; 0.215 ± 0.02 [59]; 0.21 [58]
TiC	977	920	940, 845 [62]; 929 ± 56 [59]; 947 [63]	0.24	0.22	0.187 ± 0.01 [59]; 0.17–0.19 [60]; 0.19 [66]
TiN	782	778	757 [56]	0.33	0.30	0.295 [60]; 0.254 [61][a]; 0.22 [66]
ZrC	757	703	700, 649 [62]; 699 [63]	0.26	0.19	0.191–0.257 [60]; 0.20 [66]
ZrN	691	649	683 [56]	0.30	0.25	0.186–0.25 [60]; 0.26 [66]
HfC	732	656	553, 549 [62]; 545 [63]	0.215	0.08	0.166–0.18 [60]; 0.16 [66]
HfN	609	609	–	0.30	0.14	0.259–0.35 [60]; 0.17 [66]

[a] Calculated from the elastic stiffness constants of single crystals by the VRH approximation (see Appendix A).

Table 2
Calculated elastic moduli compared with the experimental data measured at room temperature

	B (GPa)		*E* (GPa)		*G* (GPa)	
	Calculation	Experiment	Calculation	Experiment[a]	Calculation	Experiment
VC	307	–	433	255–446 [60]	171	–
VN	317	268 [61][b]	293	393 [61][b]	109	156 [61][b]
NbC	285	300 [64]	419	441, 514 [60]; 488 [64]; 478 [58]	167	198 [64]; 197 [58]
NbN	292	287 [61][b]; 292 [67][b]	307	387 [61][b]	116	152 [61][b]; 117 [67][b]
TaC	317	332 ± 39 [59]; 344 [64]	514	567 ± 68 [59]; 537 [64]; 490 [58]	209	234 ± 27 [59]; 216 [64]; 202 [58]
TiC	257	233 ± 14 [59]; 242 [66]	401	439 [60]; 436 ± 26 [59]; 445 [66]	162	184 ± 11 [59]; 187 [66]
TiN	283	277 [66]; 318 [61][b]	289	604 [60]; 463 [66]; 469 [61][b]	109	189 [66]; 187 [61][b]
ZrC	217	207 [65]; 230 [66]	312	>318 [60]; 386 [65]; 395 [66]	124	162 [65]; 165 [66]
ZrN	243	240 [66]; 216 [67][b]	292	392 [60]; 390 [66]	112	155 [66]; 138 [67][b]
HfC	236	242 [64]; 200 [66]	404	424 [60]; 461 [64]; 430 [66]	166	195 [64]; 185 [66]
HfN	267	235 [66]; 306 [67][b]	320	333 [60]; 410 [66]	123	175 [66]; 150 [67][b]

[a] Kral et al. [60] collected experimental elastic properties at various carbon or nitrogen contents, and at various porosities. Only data for stoichiometric composition and for bulk samples with smallest porosity are selected here. Data for films are generally higher than those for bulk samples, thus not used for comparison.
[b] Calculated from the elastic stiffness constants of single crystals by the VRH approximation (see Appendix A).

Table 3
The elastic moduli calculated in this work compared with the values obtained directly from ab initio calculations in the literature

	B (GPa)		*G* (GPa)	
	Present calculation by VASP	Ab initio calculation	Present calculation	Ab initio calculation[a]
VC	307	348 (FPLAPW-LDA [69])[b]	171	241 [69]
VN	317	370 [69][b]	109	168 [69]
NbC	285	331 (LDA [7])[a]; 328 (FPLAPW-LDA [68])[b]; 293 (FPLAPW-GGA [68])[b]	167	193 [7]; 222 (LDA [68]); 209 (GGA [68])
NbN	292	354 [7][a]; 350 (FPLAPW-LDA [68])[b]; 307 (FPLAPW-GGA [68])[b]	116	134 [7]; 187 (LDA [68]); 108 (GGA [68])
TaC	317	357 [7][a]	209	214 [7]
TaN	320	372 [7][a]	–	84 [7]
TiC	257	220 (FPLMTO-GGA [6])[b]; 286 [69][b]	162	175 [6]; 198 [69]
TiN	283	270 [6][b]; 326 [69][b]	109	199 [6]; 209 [69]
ZrC	217	247 [7][a]	124	177 [7]
ZrN	243	283 [7][a]	112	169 [7]
HfC	236	263 [7][a]	166	200 [7]
HfN	267	306 [7][a]	123	185 [7]

[a] Calculated from the elastic stiffness constants of single crystals by the VRH approximation (see Appendix A).
[b] Evaluated by fitting the ab initio calculated energy and volume curve.

calculations. Bulk modulus can be evaluated from ab initio calculations in two ways. One way is to fit the calculated energy and volume curve by using certain EOS. This method is adopted in the present work to calculate B. The other way is to calculate elastic constant c_{ij} and evaluate the average bulk modulus using the Voigt–Reuss–Hill approximation (see Appendix A). Young's and shear moduli are always calculated in this way in the present work.

Table 3 lists the bulk and shear moduli calculated in the present work as well as the values in the literature. It is well known that ab initio calculations using the local density approximation (LDA) overestimate the elastic moduli. The same conclusion is drawn by comparing Tables 2 and 3. For the bulk modulus, the present GGA calculations agree well with the experimental data. For shear modulus, ab initio calculations are capable of providing data within experimental uncertainty, while the calculated values in the present work are lower.

4. Conclusions

For the cubic carbides and nitrides studied in this work, the Debye–Grüneisen model using the DM approximation for γ reproduces most experimental data for heat capacity. For the case of CLE, the agreement is less satisfactory. However, considering the uncertainty of the experimental results, the DM approximation still works better than Slater's approximation.

By incorporating Poisson's ratio into the relation between Debye temperature and volume, and by comparing with the experimental heat capacity and CLE, we evaluated Poisson's ratio. Combining this further with the calculated bulk modulus, Young's and shear moduli can also be calculated. The calculated values for bulk and Young's moduli agree reasonably well with the experimental data, whereas the shear modulus is generally lower than the experimental values.

Both Poisson's ratio and mass affect the calculated heat capacity and thermal expansivity. For compounds whose constituent atoms have large difference in atomic mass, such as TaC and HfN, the use of the logarithmic averaged mass is necessary to evaluate the Debye temperature and obtain reasonable Poisson's ratios.

Acknowledgements

The work was financially supported by the Swedish Foundation for Strategic Research (SSF) and industry through the Centre for Computational Thermodynamics (CCT) and through the MATOP project. Prof. G. Grimvall and Dr. Q. Chen are gratefully acknowledged for reading the manuscript and for valuable discussions. One of the authors (X.-G.L.) thanks Dr. Y. Wang for kindly providing the program for the Debye–Grüneisen calculations and patient teaching and discussions.

Appendix A. The Voigt–Reuss–Hill approximation [30]

For cubic structures, the elastic properties of a single crystal are described by three elastic constants, c_{11}, c_{12} and c_{44}. The effective elastic moduli of isotropic polycrystals can be evaluated from the elastic constants by the following two approximations. The Voigt assumptions [30], which lead to the upper limit shown by Hill [70], are

$$B_{\mathrm{V}} = \frac{c_{11} + 2c_{12}}{3} \tag{A.1}$$

$$G_{\mathrm{V}} = \frac{c_{11} - c_{12} + 3c_{44}}{5} \tag{A.2}$$

$$v_{\mathrm{V}} = \frac{3B_{\mathrm{V}} - 2G_{\mathrm{V}}}{2(3B_{\mathrm{V}} + G_{\mathrm{V}})} \tag{A.3}$$

The Reuss assumptions [30], which set the lower limit, are

$$B_{\mathrm{R}} = B_{\mathrm{V}} = \frac{c_{11} + 2c_{12}}{3} \tag{A.4}$$

$$G_{\mathrm{R}} = \frac{5(c_{11} - c_{12})c_{44}}{4c_{44} + 3(c_{11} - c_{12})} \tag{A.5}$$

$$v_{\mathrm{R}} = \frac{3B_{\mathrm{R}} - 2G_{\mathrm{R}}}{2(3B_{\mathrm{R}} + G_{\mathrm{R}})} \tag{A.6}$$

The Voigt–Reuss–Hill (VRH) mean values [30] are

$$B_{\mathrm{VRH}} = B_{\mathrm{V}} = B_{\mathrm{R}} \tag{A.7}$$

$$G_{\mathrm{VRH}} = \frac{G_{\mathrm{V}} + G_{\mathrm{R}}}{2} \tag{A.8}$$

$$v_{\mathrm{VRH}} = \frac{v_{\mathrm{V}} + v_{\mathrm{R}}}{2} \tag{A.9}$$

References

[1] Storms EK. The refractory carbides. New York (NY): Academic Press; 1967.
[2] Toth LE. Transition metal carbides and nitrides. New York (NY): Academic Press; 1971.
[3] Zhukov VP, Gubanov VA, Jepsen O, Christensen NE, Andersen OK. J Phys Chem Solids 1988;49:841.
[4] Price DL, Cooper BR. Phys Rev B 1989;39:4945.
[5] Ahuja R, Eriksson O, Wills JM, Johansson B. Phys Rev B 1996;53:3072.
[6] Hugosson HW, Eriksson O, Jansson U, Johansson B. Phys Rev B 2001;63:134108.
[7] Wu Z, Chen XJ, Struzhkin VV, Cohen RE. Phys Rev B 2005;71:214103.
[8] Lu X-G, Selleby M, Sundman B. Acta Mater 2005;53:2259.
[9] Wang Y, Ahuja R, Johansson B. Int J Quantum Chem 2004;96:501.
[10] JANAF thermodynamic tables, 3rd ed. J Phys Chem Ref Data 1985:14 (suppl 1).
[11] Kaufman L, Bernstein H. Computer calculations of phase diagrams. New York (NY): Academic Press; 1970.
[12] Saunders N, Miodownik AP. CALPHAD (calculation of phase diagrams): a comprehensive guide. Pergamon/Elsevier Science; 1998.
[13] Touloukian YS, Kirky RK, Taylor RE, Lee TYR, editors. Thermal properties of matter, TPRC data books, vol. 13. New York (NY): Plenum Press; 1975.
[14] Pearson WB. A handbook of lattice spacings and structures of metals and alloys, vols. 1 and 2. Pergamon Press; 1958. 1967.
[15] Jansson B. TRITA-MAC 0234. Stockholm, Sweden: Royal Institute of Technology; 1984.
[16] Sundman B, Jansson B, Andersson J-O. CALPHAD 1985;9:153.
[17] Andersson J-O, Helander T, Höglund L, Shi P, Sundman B. CALPHAD 2002;26:273.
[18] Kresse G, Hafner J. Phys Rev B 1994;49:14251.
[19] Kresse G, Furthmuller J. Phys Rev B 1996;54:11169.
[20] Kresse G, Joubert J. Phys Rev B 1999;59:1758.
[21] Perdew JP, Wang Y. Phys Rev B 1992;45:13244.
[22] Perdew JP, Chevary JA, Vosko SH, Jackson KA, Pederson MR, Singh DJ, et al. Phys Rev B 1992;46:6671.
[23] Kittel C. Introduction to solid state physics. New York (NY): Wiley; 1996. p. 152.
[24] Ashcroft NW, Mermin ND. Solid state physics. Florida: Saunders College Publishing; 1976. p. 54.
[25] Zharkov VN, Kalinin VA. Equations of state for solids at high pressures and temperatures. New York (NY): Consultants Bureau; 1971.
[26] Wasserman E, Stixrude L, Cohen RE. Phys Rev B 1996;53:8296.
[27] Slater JC. Introduction to chemical physics. New York (NY): McGraw-Hill; 1939.
[28] Dugdale JS, MacDonald DKC. Phys Rev 1953;89:832.
[29] Vashchenko VY, Zubarev VN. Sov Phys Solid State 1963;5:653.
[30] Grimvall G. Thermophysical properties of materials. Amsterdam: North-Holland; 1999.
[31] Jonsson S. Z Metallkd 1996;87:703.
[32] Jonsson S. Z Metallkd 1996;87:691.
[33] Dumitrescu LFS, Hillert M, Sundman B. Z Metallkd 1999;90:534.
[34] Lengauer W, Binder S, Aigner K, Ettmayer P, Guillou A, Debuigne J, et al. J Alloys Compd 1995;217:137.
[35] Aigner K, Lengauer W, Rafaja D, Ettmayer P. J Alloys Compd 1994;215:121.
[36] Wokulska K. J Alloys Compd 1998;264:223.
[37] Dubrovinskaia NA, Dubrovinsky LS, Saxena SK, Ahuja R, Johnsson B. J Alloys Compd 1999;289:24.
[38] Guillermet AF. J Alloys Compd 1995;217:69.

[39] Bogdanov VS, Neshpor VS, Kondrashev YD, Goncharuk AB, Pityulin AN. Sov Powder Metall Metal Ceram 1982;21:412.
[40] Turchanin AG, Polyakov AE. Izv Akad Nauk SSSR Neorg Mater 1982;18:404.
[41] Lengauer W, Ettmayer P. J Less-Common Metals 1991;168:L7.
[42] Westrum EF, Sommers JA. J Thermal Anal Calorim 2002;69:103.
[43] Storms EK, Kempter CP. J Chem Phys 1965;42:2043.
[44] Lipatnikov VN, Gusev AI, Ettmayer P, Lengauer W. J Phys Condens Matter 1999;11:163.
[45] Huang W. Z Metallkd 1991;82:174.
[46] Lengauer W, Ettmayer P. Monatsh Chem 1986;117:713.
[47] Carlson ON, Smith JF, Nafziger RH. Metall Trans A 1986;17:1647.
[48] Litvinenko VF, Bolgar AS, Kas'yan VI, Shvedova LK, Timofeeva JJ. Poroshk Metall 1980;2:46.
[49] Du Y, Schmid-Fetzer R, Ohtani H. Z Metallkd 1997;88:7.
[50] Kempter CP, Storms EK. J Less-Common Met 1967;13:443.
[51] Huang W, Selleby M. Z Metallkd 1997;88:55.
[52] Gusev AI, Rempel AA, Lipatnikov VN. Phys Status Solidi B 1996;194:467.
[53] Lengauer W, Ettmayer P. Monatsh Chem 1986;117:275.
[54] Timofeeva II, Shvedova LK. Izv Akad Nauk Neorg Mater 1972;8:1169.
[55] Huang W. Metall Mater Trans A 1996;27:3591.
[56] Kutolin SA, Belova LF, Samoilova RN, Kotenko OM. Izv Akad Nauk SSSR Neorg Mater 1976;12:1585.
[57] Frisk K, Guillermet AF. J Alloys Compd 1996;238:167.
[58] Jun CK, Shaffer PTB. J Less-Common Met 1971;23:367.
[59] Dodd SP, Cankurtaran M, James B. J Mater Sci 2003;38:1107.
[60] Kral C, Lengauer W, Rafaja D, Ettmayer P. J Alloys Compd 1998;265:215.
[61] Kim JO, Achenbach JD, Mirkarimi PB, Shinn M, Barnett SA. J Appl Phys 1992;72:1805.
[62] Chang YA, Toth LE, Tyan YS. Metall Trans 1971;2:315.
[63] Ajami FI, MacCrone RK. J Less-Common Met 1974;38:101.
[64] Brown HL, Armstrong PE, Kempter CP. J Chem Phys 1966;45:547.
[65] Brown HL, Kempter CP. Phys Status Solidi 1966;18:K21.
[66] Yang Q, Lengauer W, Koch T, Scheerer M, Smid I. J Alloys Compd 2000;309:L5.
[67] Chen XJ, Struzhkin VV, Wu Z, Somayazulu M, Qian J, Kung S, et al. Proc Natl Acad Sci USA 2005;102:3198.
[68] Amriou T, Bouhafs B, Aourag H, Khelifa B, Bresson S, Mathieu C. Physica B 2003;325:46.
[69] Wolf W, Podloucky R. Philos Mag B 1999;79:839.
[70] Hill R. Proc Phys Soc Lond A 1952;65:349.